Journal of Chromatography B, 878 (2010) 2003–2012

Contents lists available at ScienceDirect

Journal of Chromatography B

journal homepage: www.elsevier.com/locate/chromb

Mining ventricular cerebrospinal fluid from patients with traumatic brain injury using hexapeptide ligand libraries to search for trauma biomarkers

Marcus O.D. Sjödin*, Jonas Bergquist, Magnus Wetterhall

Analytical Chemistry, Department of Physical and Analytical Chemistry, Uppsala University, Husargatan 3, P.O. Box 599, SE 751 24, Uppsala, Sweden

ARTICLE INFO

Article history:
Received 10 March 2010
Accepted 23 May 2010
Available online 31 May 2010

Keywords:
Cerebrospinal fluid
Hexapeptide ligand library
Traumatic brain injury
Proteomics
Mass spectrometry

ABSTRACT

Traumatic brain injury (TBI) is an acute event resulting from external force to the brain and is a major cause of death and disability associated with high health care costs in the western world. Additional injuries, originating from the secondary molecular events after the initial intensive care, may be limited by the use of objective biomarkers to provide the best treatment and patient prediction outcome. In this study, hexapeptide ligand libraries (HLL) have been used for the enrichment of suggested protein biomarkers for TBI in cerebrospinal fluid (CSF). HLL have the potential to enrich low abundant proteins and simultaneously reduce the high abundant proteins, rendering a sample with significantly reduced dynamic range. The CSF proteome from two TBI inflicted patients have been extensively mapped using a large initial sample volume obtained by extraventricular drainage. Shotgun proteomics, in combination with isoelectric focusing (IEF) and nano-LC–MS/MS, identified 339 unique proteins (MudPIT scoring $p \leq 0.05$) with a protein overlap of 130 between the patients. As much as 45% of the proteins reported in the literature to be associated with degenerative/regenerative processes occurring after a trauma to the head were identified. Out of the most prominent potential protein biomarkers, such as neuron specific enolase, glial fibrillary acidic protein, myelin basic protein, creatine kinase B-type and S-100β, all except myelin basic protein were detected in the study. This study shows the possibility of using HLL as a tool for screening of low abundant protein biomarkers in human CSF.

1. Introduction

Traumatic brain injury (TBI) is one of the leading causes of death and disability in the western world and is associated with high health care costs as a result of the acute treatment, long-term rehabilitation and loss of productivity [1]. TBI is defined as direct physical impact to the head. In the post-traumatic period, a series of complex secondary molecular events are triggered that are both degenerative and regenerative processes [2]. An inflammatory response is most prominent in the early phase (days) [3]. Additional neural cell death, occurring either through apoptosis or necrosis, is an ongoing process over a longer time span (weeks) [4]. In time (months), brain tissue remodeling occurs through synaptic plasticity and possible stem cell differentiation [2]. A complete understanding of these ongoing biological processes still remains elusive. Clinically, there is little that can be done to the initial damage caused by the trauma. However, the injuries resulting from the secondary molecular events can be therapeutically treated. Objective biomarkers to monitor the severity and to follow the treatment in the post-traumatic period would greatly improve clinical decisions and outcome. The matrix most likely to contain a measurable TBI biomarker is cerebrospinal fluid (CSF) because of its close contact with the region of injury. Studies focused on finding biomarkers for TBI in CSF have revealed several candidates with clinical potential, where neuron specific enolase (NSE), glial fibrillary acid protein (GFAP), myelin basic protein (MBP), creatine kinase B-type (CK-B) and S-100β have attracted the most attention. There is, however, currently no single clinically verified biomarker for the diagnosis of TBI. Nonetheless, the study of protein patterns in CSF could potentially provide improved outcome predictions for TBI [5]. CSF is a very complex sample matrix that contains a great number of proteins present in a large dynamic range, spanning at least 10 orders of magnitude. This is a major issue since commonly employed proteomics methods are only able to span over 4 orders of magnitude [6]. Furthermore, the total protein concentration is approximately only 0.2–0.6 mg/mL which is about 100 times lower than for plasma [7], making detection of low abundance proteins a challenging task. This is further complicated by the fact that 99% of the total protein content is

Abbreviations: HLL, hexapeptide ligand libraries; TBI, traumatic brain injury; CSF, cerebrospinal fluid; IEF, isoelectric focusing; ESI, electrospray; LC–MS/MS, liquid chromatography–tandem mass spectrometry.

* Corresponding author. Tel.: +46 18 471 3673; fax: +46 18 4713 692.
E-mail address: marcus.sjodin@kemi.uu.se (M.O.D. Sjödin).

1570-0232/$ – see front matter © 2010 Elsevier B.V. All rights reserved.
doi:10.1016/j.jchromb.2010.05.036

represented only by about 20 proteins where human serum albumin (HSA) alone occupy 50–60% of the total protein content [8]. These few high abundant proteins limit the sample loading capabilities of medium and low abundant proteins and often mask the remaining trace of these proteins in both 2D PAGE (large overlapping spots) and LC–MS/MS (signal suppression). Upstream sample pretreatment is thus a necessity when analyzing CSF. Immunoaffinity based depletion is a technique that has grown over the last decade in proteomic studies of CSF with great success [9]. However, this approach is not adoptable without considerations. Since HSA is a carrier protein, other non-targeted proteins may also be co-depleted [10].

In recent years, combinatorial peptide ligand libraries have emerged as a promising tool for the capture and enrichment of proteins in biological extracts [11]. The libraries are constructed in a synthetic way and consist of millions of beads, with each bead containing a single peptide. Characteristics of these libraries are that the peptides: (1) all have the same length, (2) the combination of amino acids represent all possible combinations and (3) are present in roughly equimolar proportions. The obtained library thus comprises millions of affinity baits, which statistically should act as possible binders to each single protein present in a biological fluid. This feature makes it particularly suitable for proteomes with a large dynamic range [12]. The levels of high-abundance proteins will be reduced as these sites will quickly be saturated. However, low abundance proteins will be concentrated until the point of saturation is reached or until they are totally bound to the ligands. As the amount of affinity ligands is present in equimolar proportions, the concentration of all the captured proteins should theoretically also be the same. The excessive unbound proteins are washed away and the remaining bound proteins are eluted to yield a sample mixture where the overall dynamic range has been greatly reduced. Recent proteomic investigations using peptide combinatorial libraries have been performed on vast different proteomes [13–16]. A common feature of these studies is the unambiguous detection of a larger number of proteins compared to unprocessed samples [6].

In this study, we have explored the possibility to mine the human CSF proteome by the commercially available hexapeptide ligand library (HLL) ProteoMiner™, using a very large sample volume of CSF from patients with TBI. The large sample volume will, in theory, enable the detection down to the very low abundant proteins. As protein biomarkers are generally expected to exist in low abundance [17], we hypothesized that new insights into the pathology may arise from this. A volume as large as 150 mL from two TBI patients each was obtained for the study. The objective of the study was to explore the potential for HLL to (1) give new insights of the TBI proteome – by using a new sample preparation technique and by looking deep into the proteome, (2) establish a confident list with proteins occurring over a wide dynamic range and (3) explore the capability of HLL to detect the many currently reported potential biomarkers of TBI.

2. Experimental

2.1. Materials

Acetonitrile (ACN), formic acid (FA), acetic acid (HAc) and ammonium-di-hydrogen phosphate ($NH_4H_2PO_4$) were obtained from Merck (Darmstadt, Germany). Iodoacetamide (IAA), urea, ammonium hydrogen carbonate (NH_4HCO_3), dithiothreitol (DTT) and trifluoroacetic acid (TFA) were obtained from Sigma–Aldrich (St. Louis, MO, USA). Trypsin was of sequence-grade from Roche Diagnostics (Basel, Switzerland). All water used was Milli-Q ultrapure (Millipore, Bedford, MA, USA).

2.2. CSF preparation

The Proteominer™ kit is designed for 1 mL human plasma that has a protein concentration of 50–80 mg/mL, which is at least 100 times higher than in CSF. Hence, a large initial CSF sample volume is necessary in order to reach the required protein concentration of 50 mg/mL as stated by the manufacturer. Ventricular CSF drainage from two TBI patients, each with an approximate volume of 150 mL was collected and stored in −80 °C until further analysis. The crude CSF was thawed and aliquoted into 50 mL Falcon polypropylene tubes (BD Biosciences, San Jose, CA, USA) and refrozen over night at −80 °C. The CSF aliquots were then freeze dried at −110 °C until dryness using a Coolsafe™ vacuum concentrator (ScanVac, Lynge, Denmark). The freeze dried samples were reconstituted with water to give a total volume of 16 mL and desalted using Amicon Ultra-4 (cut-off 3 kDa) spin filters (Millipore Bedford, MA, USA). Four spin filters were first washed with 4 mL of 20 mM NH_4HCO_3. 4 mL of reconstituted CSF were then added to each spin filter and centrifuged for 20 min at 7500 × *g*. The ultrafiltrates were discarded. The retentates from each spin filter were washed with 3 mL of 20 mM NH_4HCO_3 a total of 5 times for 20 min at 7500 × *g*. The desalted retentates were recovered by pipetting the liquids into new collection tubes. Particulates were removed by centrifuging the collection tubes at 10,000 × *g* for 10 min and then pipetting the supernatants into Eppendorf low-protein binding vials (Eppendorf, Hamburg, Germany). The supernatants were pooled giving a final set of two Eppendorf vials containing approximately 1 mL each.

2.3. Bradford protein assay

The total protein content was estimated on aliquots taken throughout the sample preparation with Bradford Coomassie® Brilliant Blue G-250 protein assay using bovine serum albumin (BSA) as standard (Bio-Rad, Hercules CA, USA). The absorbance was measured using a Bio-Rad Model 680 microplate reader at 595 nm. R^2 coefficients were 0.99 or higher for all calibration curves.

2.4. ProteoMiner™ sample processing

The concentrations of the samples were determined to have a concentration of 51 mg/mL and 87 mg/mL, thus meeting the requirements of having a concentration ≥ 50 mg/mL necessary for using the ProteoMiner™ large-capacity kit. One Proteominer column was used for each sample. The centrifugation speed at all steps was 1000 × *g*. The sample preparation was carried out according to the manufacturer's instructions. The bound proteins were eluted with a buffer containing detergents and a high salt content, which needed to be removed before further processing. For this purpose, Microcon® YM-3 spin filters (Millipore) were used. Initially, the spin filters were washed with 0.5 mL of water for 20 min at 10,000 × *g*. The samples were diluted to 0.5 mL with 20 mM NH_4HCO_3 and added to the spin filters followed by centrifugation for 140 min at 10,000 × *g*. The retentates were washed with 0.5 mL of 20 mM NH_4HCO_3 a total of 2 times for 140 min at 10,000 × *g*. The filters were turned upside down and the retentates were collected into new sample reservoirs by centrifuging for 3 min at 1000 × *g*.

2.5. 1D gel electrophoresis

1D gel electrophoresis was performed on the concentrated crude CSF, the Proteominer flow-through (FT) and bound (B) fractions to visually examine the effect of the sample preparation. The total amount of protein for the 1D gels was normalized to 20 μg of each sample and dried using a SpeedVac® ISS110 (Thermo Scientific, Waltham, MA, USA). 1D gel electrophoresis was performed with a Criterion XT™ system using precast Criterion XT 18 well

4–12% Bis-Tris gels with XT MOPS running buffer (Bio-Rad). The samples were redissolved in 12.5 μL XT sample buffer, 27.5 μL MQ water and 5 μL 45 mM DTT. The samples were heated to 95 °C for 5 min, cooled to room temperature and 5 μL 100 mM IAA was added. A volume of 25 μL corresponding to 10 μg total protein was loaded in each well onto duplicate gels. The gels were run at 200 V constant for 60 min (starting current 165–175 mA/gel, final current 60–70 mA/gel). Finally, the gels were visualized by Coomassie Blue R-250 (Bio-Rad) according to the manufacturer's instructions.

2.6. In-solution tryptic digestion

Aliquots of the Proteominer™ bound fractions, corresponding to 580 and 280 μg total protein respectively, were dried down using a speedvac and redissolved in 100 μL of digestion buffer (8 M urea and 400 mM NH_4HCO_3). The proteins were reduced by adding 10 μL of 45 mM DTT and incubation for 15 min at 50 °C, where after alkylation was performed by adding 10 μL of 100 mM IAA at room temperature for 15 min in darkness. Trypsin (2.5%, w/w) was added and the samples were digested over night at 37 °C.

2.7. Sample desalting

The digested sample was diluted to a volume of 500 μL with 2.5% HAc (v/v) and desalted on a Isolute C18(EC) (1 mL, 50 mg capacity, Biotage, Uppsala, Sweden) SPE column using the following schedule: the column was first wetted with 1 mL 100% ACN and equilibrated with 5× 1 mL 1% HAc. The tryptic peptides were adsorbed to the media using 5 repeated cycles of sample loading. The column was washed using 5× 1 mL of 1% HAc and finally the peptides were eluted in 400 μL 50% ACN, 1% HAc. The aliquots were vacuum centrifuged to dryness.

2.8. OFFGEL isoelectric focusing

A 3100 OFFGEL Fractionator system (Agilent Technologies, Waldbronn, Germany) was used for in-solution isoelectric focusing (IEF) of the tryptic peptides. The IEF was conducted with the OFFGEL pH 3–10 12-well setup kit according to the manufacturer's protocol. The desalted samples were reconstituted with 1.8 mL of rehydration solution and 150 μL was loaded into each well. The IEF was conducted at a maximum 50 μA/strip until 20 kVh was reached (approximately after 12 h). After the isoelectric focusing, the solution was removed from each well and diluted to give a final volume of 0.5 mL with water containing 2.5% HAc (v/v). Each of the 12 fractions was then desalted with SPE as described previously. The desalted fractions were dried down in a speedvac, redissolved in 10 μL of solvent 1A (see nano-LC–ESI-MS/MS) and transferred to a 100 μL insert (Agilent) for nano-LC–ESI-MS/MS analysis.

2.9. Nano-LC–ESI-MS/MS analysis

The separation was performed using a Tempo nanoLC-1D plus™ (Applied Biosystems, USA) system. A volume of 3 μL of each sample was injected into a 10 μL loop in injection pickup mode. The samples were loaded onto a Peptide CapTrap (Michrom Bioresources, CA, USA) for 5 min at 15 μL/min isocratically (solvent 1A: H_2O/ACN/FA 97.9/2/0.1, v/v%). The peptides were then eluted onto a BioBasic-C18 column 5 μm × 15 cm × 75 μm (Thermo) using a stepwise gradient (solvent 2A: H_2O/ACN/FA 97.9/2/0.1 (v/v%); solvent 2B: H_2O/ACN/FA 2/97.9/0.1, v/v%) at a flow rate of 350 nL/min. The gradient was as follows: 2% B during 20 min, 2% → 8% B in 5 min, 8% → 32% B in 86 min, 32% → 40% B in 5 min and finally 40% → 80% B in 1 min. After washing for 4 min the column was equilibrated for the next sample by going from 80% → 2% B in 5 min and kept at 2% B during 14 min giving a total run time of 140 min. The samples were kept in the autosampler at 10 °C. Data was collected in positive ESI mode on a 3200 QTrap™ hybrid triple quadrupole/linear ion trap (Applied Biosystems/MDS Sciex, Canada) equipped with a MicrolonSpray II® head with an uncoated 10 μm i.d. PicoTip® (New Objective, MA, USA) as electrode. The source parameters were: ion spray voltage, 2500 V; curtain gas, 20 psi; gas 1, 20 psi; interface heater temperature, 150 °C. Spectra were acquired in automated mode using Information Dependent Acquisition (IDA). Precursors were selected by using an Enhanced Mass Scan (EMS) as a survey scan (fill time 25 ms, m/z 400–1400, 4000 amu/s). On the five most intense precursor ions, an Enhanced Resolution scan (ER) was employed for charge state determination (dynamic fill time, m/z range 30 amu, 250 amu/s) as well as an Enhanced Product Ion scan (EPI) for MS/MS data (fill time 200 ms, m/z 100–1400, 4000 amu/s). The precursor ions were fragmented by collision induced dissociation (CID) in the Q2 collision cell. Collision voltages were automatically adjusted based on the ion charge state and mass using rolling collision energy. Generated fragments ions were captured and their masses analyzed in the Q3 linear ion trap. The IDA data acquired was processed in Analyst 1.4.2 and subjected for automatic protein identification using MASCOT Daemon (version 2.2.2, Matrix Science, UK) against the SwissProt database version 51.6. The search parameters were set to Taxonomy: Homo Sapiens, Enzyme: Trypsin, Fixed modifications: Carbamidomethyl (C), Variable modifications: Oxidation (M), Peptide tolerance: 1.5 Da, MS/MS tolerance: 0.6 Da and maximum 1 missed cleavage site. The false discovery rates were automatically calculated by enabling the decoy function. Proteins were considered to be positively matched using the more stringent MudPIT scoring ($p \leq 0.05$) and the require bold red option was chosen.

3. Results and discussion

The large dynamic range, the complexity and the presence of a few high abundant proteins in CSF are of major analytical concern when studying the entire proteome. The limit of detection for all analytical techniques are restricted by the sample loading capacity. This, in turn, is a major issue for the study of low abundant species in such a complex matrix as human CSF. Therefore, sample preparation and fractionation is crucial for the outcome of the analysis. The results from the 1D gel electrophoresis are shown in Fig. 1. Hardly any difference can be noticed in the crude CSF compared to the flow-through fractions of the CSF. This is to be expected as there is only a small amount of affinity ligands in relation to the high sample load. The binding capacity of the beads is in the order of approximately 1 mg, which is only 2% or less than the sample amount in the crude CSF starting material (51 and 87 mg/mL respectively) and consequently 98% of the total protein amount will remain in the unbound CSF fraction. Hence, the majority of the total protein amount is washed away and found in the flow-through fraction. However, this fraction will mostly contain album and the other high abundant proteins in CSF that are only slightly decreased in concentration, while the medium and low abundant proteins in CSF should be concentrated in the bound fraction. The bands visualized in both bound fractions show many new, clear and distinct bands compared to the unbound fractions supporting that both the reduction of the high abundant proteins and, mostly important, the enrichment of the medium and low abundant proteins have worked properly in both samples. The number of bands in the bound fraction of the first sample is greater than for the bound fraction of the second sample, which would indicate a more proper sample preparation in the first case. This is further strengthened by the fact that the albumin band in the second bound fraction is still quite prominent. Any differences between the bound fractions of the samples also reflect the fact that they are two biological replicates so a dif-

Table 1
List of overlapping proteins from the two samples using MudPIT scoring ($p \leq 0.05$).

#	Protein name	Database entry[a]	Accession[b]	M_w[c]	Primary function[d]	Indicator of trauma[e]	Mascot score[f]	MudPit/total identified peptides[g]
Cell proliferation/commmunication/signal transduction								
1	Gelsolin	GELS	P06396	86,043	Actin modulating		580	15/39
2	Pigment epithelium-derived factor	PEDF	P36955	46,484	Differentiation/inhibitor		276	9/16
3	Lipopolysaccharide-binding protein	LBP	P18428	53,384	Immune response	Acute phase	204	3/15
4	Amyloid beta A4 protein	A4	P05067	86,943	Multiple functions	Apoptosis	105	2/23
5	Amyloid-like protein 1	APLP1	P51693	72,176	Multiple functions	Apoptosis	87	2/18
6	14-3-3 protein epsilon	1433E	P62258	29,174	Regulatory functions	Apoptosis	87	3/11
7	14-3-3 protein sigma	1433S	P31947	27,774	Regulatory functions		65	2/12
Coagulations factors								
8	Fibrinogen beta chain	FIBB	P02675	56,577	Cell proliferation		659	21/41
9	Fibrinogen gamma chain	FIBG	P02679	52,106	Cell proliferation		434	12/26
10	Prothrombin	THRB	P00734	71,475	Acute phase response	Inflammation/wound healing	351	9/20
11	Fibrinogen alpha chain	FIBA	P02671	95,656	Cell proliferation		209	8/25
12	Coagulation factor V	FA5	P12259	251,671	Regulator of hemostasis		457	10/52
13	Heparin cofactor 2	HEP2	P05546	57,071	Blood coagulation		149	9/27
Complement factors								
14	Complement C3	CO3	P01024	188,569	Immune response	Inflammatory response	3067	87/147
15	Complement factor H	CFAH	P08603	139,070	Complement activation	Inflammatory response	935	31/55
16	Complement component C9	CO9	P02748	63,173	Complement activation	Constituent of the membrane attack complex	320	11/25
17	Complement component C8 beta chain	CO8B	P07358	67,047	Complement activation	Constituent of the membrane attack complex	160	5/14
18	C4b-binding protein alpha chain	C4BP	P04003	67,033	Complement activation	Inflammatory response	150	4/14
19	Complement C1q subcomponent subunit C	C1QC	P02747	25,774	Complement activation	Inflammatory response	147	3/10
20	Complement factor H-related protein 1	FHR1	Q03591	37,651	Complement activation	Inflammatory response	129	3/8
21	Complement factor B	CFAB	P00751	85,533	Complement activation	Inflammatory response	113	3/17
22	Complement C5	CO5	P01031	188,331	Complement activation	Constituent of the membrane attack complex	83	3/32
23	Complement component C7	CO7	P10643	93,518	Complement activa-tion/defense	Constituent of the membrane attack complex	44	1/21
24	Complement C1r subcomponent	C1R	P00736	80,174	Complement factor C1 activity	Inflammatory response	43	1/10
Immune response/defense								
25	Myeloperoxidase	PERM	P05164	83,869	Enzyme activity	Anti-apoptosis	465	16/40
26	Monocyte differentiation antigen CD14	CD14	P08571	40,076	Inflamatory response	Inflammatory response	393	9/16
27	Ig alpha-1 chain C region	IGHA1	P01876	38,486	Immune response	Inflammatory response	372	7/15
28	Ig gamma-1 chain C region	IGHG1	P01857	36,596	Immune response	Inflammatory response	364	8/17
29	Ig mu chain C region	IGHM	P01871	49,307	Immune response	Inflammatory response	340	10/24
30	Ig alpha-2 chain C region	IGHA2	P01877	36,508	Immune response	Inflammatory response	333	5/12
31	Ig kappa chain C region	IGKC	P01834	11,773	Immune response	Inflammatory response	299	6/8
32	Lysozyme C	LYSC	P61626	16,537	Bacteriolytic function	Inflammatory response	187	6/12
33	Ig gamma-4 chain C region	IGHG4	P01861	35,941	Immune response	Inflammatory response	158	4/14

Table 1 (*Continued*)

#	Protein name	Database entry[a]	Accession[b]	M_w[c]	Primary function[d]	Indicator of trauma[e]	Mascot score[f]	MudPit/total identified peptides[g]
34	Serum amyloid A protein	SAA	P02735	13,532	Acute phase	Acute phase	155	4/10
35	Ig gamma-3 chain C region	IGHG3	P01860	32,331	Immune response	Inflammatory response	154	4/16
36	Ig gamma-2 chain C region	IGHG2	P01859	35,885	Immune response	Inflammatory response	137	3/14
37	Ig kappa chain V-I region AG	KV101	P01593	11,992	Immune response	Inflammatory response	132	3/3
38	Serum amyloid P-component	SAMP	P02743	25,387	Acute phase	Acute phase	130	2/3
39	Serum amyloid A-4 protein	SAA4	P35542	14,807	Acute phase	Acute phase	126	4/8
40	N-acetylmuramoyl-L-alanine amidase	PGRP2	Q96PD5	62,217	Immune response		103	3/11
41	Ig heavy chain V-III region BRO	HV305	P01766	13,227	Immune response	Inflammatory response	99	1/5
42	Ig lambda chain C regions	LAC	P01842	11,237	Immune response	Inflammatory response	87	2/6
43	Ficolin-3	FCN3	O75636	32,903	Immune response		73	2/4
44	Immunoglobulin J chain	IGJ	P01591	18,099	Immune response	Inflammatory response	72	2/5
45	Ig heavy chain V-III region TIL	HV304	P01765	12,356	Immune response	Inflammatory response	56	1/3
46	Stromal cell-derived factor 1	SDF1	P48061	10,666	Regulatory function		36	1/2
47	Azurocidin	CAP7	P20160	26,886	Regulatory function	Inflammatory response	32	1/4
Metabolism/enzymes and inhibitors								
48	Apolipoprotein E	APOE	P02649	36,154	Lipid metabolism	Anti-apoptosis	1169	22/40
49	Ceruloplasmin	CERU	P00450	188,569	Iron transport, enzyme activity		1163	26/46
50	Apolipoprotein A-IV	APOA4	P06727	45,399	Lipid metabolism		521	17/33
51	Alpha-1-antitrypsin	A1AT	P01009	46,878	Inhibitor/immune respons	Acute phase response	470	11/25
52	Alpha-2-macroglobulin	A2MG	P01023	164,600	Inhibitor	Tumor necrosis factor binding/interleukin 1/8-binding	459	18/43
53	Alpha-enolase	ENOA	P06733	47,169	Multifunctional enzyme		288	7/28
54	Inter-alpha-trypsin inhibitor heavy chain H4	ITIH4	Q14624	103,357	Acute phase	Acute phase	284	8/30
55	Dickkopf-related protein 3	DKK3	Q9UBP4	38,291	Inhibitor of Wnt signaling pathway		240	6/6
56	Sulfhydryl oxidase 1	QSCN6	O00391	82,578	Oxidation of sulfhydryl groups		240	6/22
57	Glutathione peroxidase 3	GPX3	P22352	25,552	Enzyme activity		229	7/12
58	Plasminogen	PLMN	P00747	90,569	Blood coagulation	Factor in inflammation	222	7/21
59	Vitronectin	VTNC	P04004	55,069	Cell adhesion/inhibitor		203	6/16
60	Glyceraldehyde-3-phosphate dehydrogenase	G3P	P04406	36,053	Enzyme activity in glycolysis		201	5/14
61	Cystatin-C	CYTC	P01034	15,799	Enzyme regulator	Cerebral hemorrhage and premature stroke	185	5/15
62	Carboxypeptidase E	CBPE	P16870	53,151	Enzyme activity		169	6/13
63	Cathepsin D	CATD	P07339	44,552	Enzyme activity	Cell death	157	5/15
64	Prostaglandin-H2 D-isomerase	PTGDS	P41222	21,029	Catalytic activity	Possible anti-apoptotic role	150	3/4
65	ProSAAS	PCSK1	Q9UHG2	27,372	Inhibitor		141	2/13
66	14-3-3 protein gamma	1433G	P61981	28,303	Multiple regulatory functions	Anti-apoptosis	141	4/13
67	14-3-3 protein zeta/delta	1433Z	P63104	27,745	Multiple regulatory functions	Anti-apoptosis	131	4/15
68	Pyruvate kinase isozymes M1/M2	KPYM	P14618	57,937	Glycotic enzyme		128	3/24

Table 1 (*Continued*)

#	Protein name	Database entry[a]	Accession[b]	M_w[c]	Primary function[d]	Indicator of trauma[e]	Mascot score[f]	MudPit/total identified peptides[g]
69	Peroxiredoxin-2	PRDX2	P32119	21,892	Cell redox homeostasis	Anti-apoptosis/signaling tumor necrosis factor alpha	126	5/13
70	Metalloproteinase inhibitor 1	TIMP1	P01033	23,171	Inhibitor		94	2/3
71	Eosinophil peroxidase	PERE	P11678	81,040	Enzyme activity		91	2/22
72	L-Lactate dehydrogenase A chain	LDHA	P00338	36,689	Glycotic enzyme		91	3/14
73	Creatine kinase B-type	KCRB	P12277	42,644	Enzyme activity		85	2/13
74	Procollagen C-endopeptidase enhancer 1	PCOC1	Q15113	47,972	Enzyme activity		84	2/7
75	Peroxiredoxin-6	PRDX6	P30041	25,035	Cell redox homeostasis		75	3/11
76	Alpha-2-antiplasmin	A2AP	P08697	54,566	Inhibitor activity	Acute phase response	75	2/9
77	Serum paraoxonase/arylesterase 1	PON1	P27169	39,749	Enzyme activity		75	2/11
78	Phosphoglycerate kinase 1	PGK1	P00558	44,615	Glycotic enzyme		69	1/17
79	Kininogen-1	KNG1	P01042	72,996	Inhibitor	Inflammatory response	69	1/18
80	L-Lactate dehydrogenase A-like 6B	LDH6B	Q9BYZ2	41,943	Glycotic enzyme		58	1/13
81	Apolipoprotein C-III	APOC3	P02656	10,852	Inhibit lipases		52	1/8
82	Probable serine carboxypeptidase CPVL	CPVL	Q9H3G5	54,164	Probable proteolytic activity	Inflammatory response	50	1/13
83	Protein-L-isoaspartate	PIMT	P22061	24,650	Enzyme activity		49	1/7
84	6-Phosphogluconate dehydrogenase	6PGD	P52209	53,140	Enzyme activity		48	1/6
85	Myosin light polypeptide 6	MYL6	P60660	16,930	Regulatory funcion		44	1/6
86	Antithrombin-III	ANT3	P01008	52,602	Serine protease inhibitor		44	1/17
87	Ribonuclease 4	RNAS4	P34096	16,840	Nucleotide specificity		39	1/5
Miscellaneous								
88	Clusterin	CLUS	P10909	53,031	Apoptosis	Apoptosis	1132	26/30
89	Vimentin	VIME	P08670	53,652	Protein binding/structural constituent		437	11/29
90	Alpha-1-antichymotrypsin	AACT	P01011	47,651	Probable inhibitor	Increases in the acute phase of inflammation	221	4/14
Structural/membrane associated/extracellular matrix								
91	Fibronectin	FINC	P02751	266,034	Cell structure	Acute phase/wound healing	923	25/56
92	Fibulin-1	FBLN1	P23142	77,261	Extracellular matrix protein		861	21/30
93	Actin, cytoplasmic 1	ACTB	P60709	41,737	Cell motility		489	14/25
94	Galectin-3-binding protein	LG3BP	Q08380	65,331	Cell adhesion		364	9/21
95	Periostin	POSTN	Q15063	93,314	Cell adhesion		324	9/29
96	Apolipoprotein A-II	APOA2	P02652	11,175	Stabilization of HDL		235	7/12
97	Mimecan	MIME	P20774	33,922	Bone formation		158	5/11
98	Actin, alpha skeletal muscle	ACTS	P68133	42,051	Cell motility		134	7/20
99	Microfibril-associated glycoprotein 4	MFAP4	P55083	28,648	Cell adhesion		86	2/4
100	Glial fibrillary acidic protein	GFAP	P14136	49,880	Intermediate filament	Acute phase	84	5/27
101	Vacuolar ATP synthase subunit S1	VAS1	Q15904	52,026	Proton transport		77	2/17
102	Transforming growth factor-beta-induced protein ig-h3	BGH3	Q15582	74,681	Cell adhesion		71	2/16
103	Chloride intracellular channel protein 1	CLIC1	O00299	26,923	Ion transport		66	1/10
104	Thrombospondin-1	TSP1	P07996	129,383	Cell adhesion	Anti-apoptosis/apoptosis	63	1/17
105	Coronin-1A	COR1A	P31146	51,026	Actin binding		42	1/5
Transport/binding								
106	Apolipoprotein B-100	APOB	P04114	515,563	Lipid metabolism		1641	60/172

Table 1 (*Continued*)

#	Protein name	Database entry[a]	Accession[b]	M_w[c]	Primary function[d]	Indicator of trauma[e]	Mascot score[f]	MudPit/total identified peptides[g]
107	Hemoglobin subunit beta	HBB	P68871	15,998	Oxygen transport		1390	19/22
108	Serum albumin	ALBU	P02768	71,317	Transport		1348	37/57
109	Apolipoprotein A-I	APOA1	P02647	30,759	Cholesterol transport	Inhibition of interleukin-1 beta secretion	1284	26/40
110	Hemoglobin subunit delta	HBD	P02042	16,055	Oxygen transport		849	16/19
111	Hemoglobin subunit alpha	HBA	P69905	15,258	Oxygen transport		735	14/19
112	EGF-containing fibulin-like extracellular matrix protein 1	FBLN3	Q12805	54,641	Ca binding		465	15/19
113	Transthyretin	TTHY	P02766	15,991	Hormone transport		261	6/9
114	Apolipoprotein D	APOD	P05090	21,276	Transport		219	7/14
115	Collagen alpha-3(VI) chain	CO6A3	P12111	343,665	Cell adhesion		168	5/67
116	Lactotransferrin	TRFL	P02788	78,182	Iron transport		161	5/19
117	Nucleobindin-1	NUCB1	Q02818	53,879	Ca binding protein of the Golgi		144	4/14
118	Haptoglobin	HPT	P00738	45,861	Iron homeostasis, metabolism	Acute phase	143	5/15
119	Inter-alpha-trypsin inhibitor heavy chain H2	ITIH2	P19823	106,436	Transport/binding		130	2/23
120	Histone H2B type 1-M	H2B1M	Q99879	13,989	DNA-binding		129	3/11
121	Vitamin D-binding protein	VTDB	P02774	52,964	Transport/cell communication		123	5/17
122	Apolipoprotein C-II	APOC2	P02655	11,284	Lipid transport		110	3/6
123	Serotransferrin	TRFE	P02787	79,280	Iron transport		108	4/24
124	Alpha-actinin-1	ACTN1	P12814	103,058	Cell motility	Regulator of apoptosis	106	2/25
125	Insulin-like growth factor-binding protein 7	IBP7	Q16270	29,130	IGF binding protein		105	4/9
126	Lumican	LUM	P51884	38,429	Binds to Laminin		87	3/12
127	Histone H4	H4	P62805	11,367	DNA-binding		85	3/6
128	Hemopexin	HEMO	P02790	52,385	Binds and transport heme	Acute phase	61	3/9
129	Apolipoprotein C-I	APOC1	P02654	9332	Lipid transport		61	3/5
130	Ferritin light chain	FRIL	P02792	20,020	Iron storage		53	1/10

[a] Uniprot knowledgebase entry.
[b] Primary accession number from Uniprot knowledgebase.
[c] Molecular weight in Dalton.
[d] Primary function as listed in Uniprot.
[e] Protein function associated with degenerative or regenerative processes as listed in Uniprot.
[f] The total mascot protein score by employing MudPit scoring at a significance level at $p \geq 0.95$. At these settings, only peptides with an individual ion score ≥ 32 contributed to the total protein score.
[g] Ratio of identified peptides with an ion score ≥ 32 and total number of identified peptides corresponding to the protein.

ference between the bound fractions is to be expected because of natural biological variation. Additionally, some experimental error is also to be expected due to the many sample preparation steps prior to the analysis where, for example, proteolytic breakdown can occur. Considering the differences, the number of identified proteins by MS in the bound fraction of the second processed sample would be expected to be lower, which was also the case. The nano-LC–ESI-MS/MS analysis of the IEF fractions using the strict MudPIT 95% confidence scoring criteria described earlier rendered in a total of 1583 and 851 matched peptides corresponding to 265 and 204 proteins in the first and second sample. 130 of the proteins occurred in both samples and thereby yielding a total of 339 unique proteins identified in the CSF samples as visualized in a Venn diagram in Fig. 2(A). The false discovery rates were found to be at acceptable values of 3.03% and 3.06% respectively. The complete matched protein sets (MudPIT scoring $p \leq 0.05$) are listed in Supplementary Table 1. The *Human Proteomics Organisation* (HUPO) has published general guidelines on how proteomics data should be interpreted and presented. This is summarised in the Proteomics Standards Initiative (http://www.psidev.info). These initiatives are of great importance in order to compare data from different studies conducted by different research groups. However, these are merely guidelines on how to report data and do not specify what is to be considered a significant match. In summary, there is still no golden standard that is generally accepted on how to report data and what is to be considered a significant match. This is reflected in the literature where different research groups report a vast difference in the number proteins identified (only a few hundreds up to several thousands) despite using the same sample matrix, similar preparation procedures, similar sample volumes, the same separation techniques and identical mass spectrometers. The settings for the search criteria are crucial for the number of proteins identified in a sample. This can easily be illustrated by changing a few settings from our obtained results. The require bold red option is a way to remove duplicate homologous proteins, where red indicates that every protein includes at least one top scoring peptide match for a given spectrum and bold that it is the first time a match to a given spectrum is appearing in the report. So, if a protein hit

Table 2
Biomarkers for TBI in human CSF and brain tissue.

Protein	Accession	Regulation	Matrix	Detected in sample 1/2	Refs.
Haptoglobin	P00738	↑	CSF	Yes/Yes	[24]
Prostaglandin D2 synthase	P41222	↑	CSF	Yes/Yes	[24]
Cystatin-C	P01034	↑	CSF	Yes/Yes	[24]
Apolipopoprotein E	P02649	↓	CSF	Yes/Yes	[31]
Amyloid β-protein	P05067	↓	CSF	Yes/Yes	[31]
α1-antitrypsin	P01009	↑	CSF	Yes/Yes	[23]
Matrix metalloproteinase-9	P14780	↑	CSF	No/No	[25]
Nerve growth factor	P01138	↑	CSF	No/No	[22]
C-reactive protein	P02741	↑	CSF	Yes/No	[30]
Tumor necrosis factor-α	P01375	↑	CSF	No/No	[30]
Interleukin 1-β	P01584	↑	CSF	No/No	[22]
Interleukin 6	P05231	↑	CSF	No/No	[35]
Interleukin 8	P10145	↑	CSF	No/No	[28]
P-Selectin	P16109	↑	CSF	No/No	[37]
ICAM-1	P05362	↑	CSF	No/No	[37]
Bcl-2	P10415	↑	CSF	No/No	[36]
Caspase-3	P42574	↑	CSF	No/No	[36]
sFas	P48023	↑	CSF	No/No	[36]
Procalcitonin	P01258	↑	CSF	No/No	[26]
Cytochrome C	P99999	↑	CSF	No/No	[32]
Neuron specific enolase	P09104	↑	CSF	Yes/No	[21]
S-100β	P04271	↑	CSF	Yes/No	[33]
Myelin basic protein	P02686	↑	CSF	No/No	[21]
14-3-3 Protein[a]	–	↑	CSF	Yes/Yes	[34]
αII-spectrin	Q13813	↑	CSF	No/No	[34]
Ubiquitin hydrolase L1	P09936	↑	CSF	No/No	[34]
Creatine kinase B-type	P12277	↑	CSF	Yes/Yes	[29]
Glial fibrillary acidic protein	P14136	↑	Brain tissue	Yes/Yes	[27]
Complement component 1q	P02746	↑	Brain tissue	Yes/Yes	[20]
Complement component 3b	P01024	↑	Brain tissue	Yes/Yes	[20]
Complement component 3d	P01024	↑	Brain tissue	Yes/Yes	[20]
Membrane attack complex[b]	–	↑	Brain tissue	Yes/Yes	[20]
Clusterin	P10909	↑	Brain tissue	Yes/Yes	[20]

[a] Several isoforms exist of the 14-3-3 family.
[b] The membrane attack complex is composed of several complement factors.

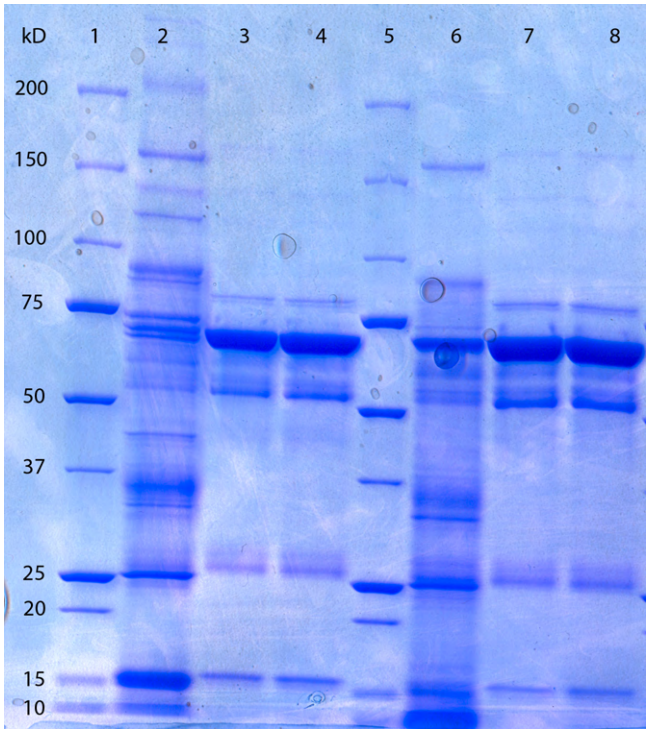

Fig. 1. 1D gel of the fractions from the Proteominer™ depletion. An amount of was loaded onto each well. Wells 2–4 are from the first sample and 6–8 from the second sample. The wells, from left to right are as follows: (1) marker (2) bound (3) flow-through (4) crude CSF (5) marker (6) bound (7) flow-through (8) crude CSF.

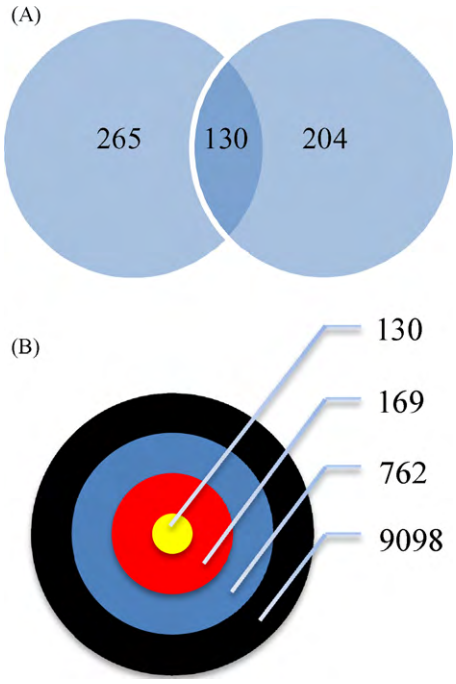

Fig. 2. (A) Venn diagram showing the identified and overlapping proteins using the most stringent search criteria–MudPit scoring $p \leq 0.05$ and require bold red. (B) A bulls eye plot showing the identified and overlapping proteins employing different search criteria. (130) MudPit scoring $p \leq 0.05$ and require bold red, (169) MudPit scoring $p \leq 0.05$, (762) Standard scoring $p \leq 0.05$ and require bold red, (9098) Standard scoring $p \leq 0.05$. (For interpretation of the references to colour in this figure legend, the reader is referred to the web version of the article.)

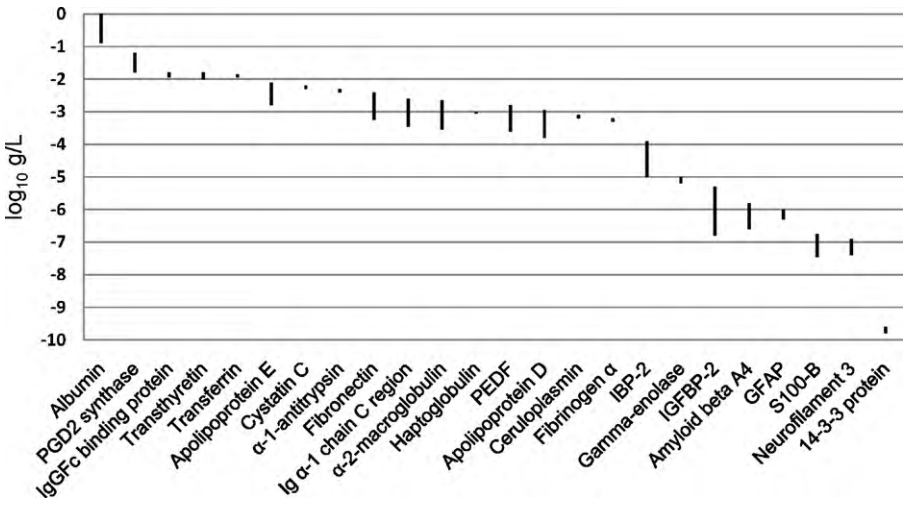

Fig. 3. Comparison of reference concentration ranges in normal human CSF for 24 identified proteins from both samples.

does not have a bold red match, then another assigned spectrum have better scoring peptides elsewhere in the list. By disabling this option, 315 and 215 proteins could be identified in the first and second sample with 169 proteins overlapping in both fractions. An even larger discrepancy can be found by changing the search criteria from MudPIT to standard scoring. The MudPIT scoring is more stringent in that it only includes peptides with MS/MS ion scores passing the significance threshold. The total protein MASCOT ion score is a weighted function of the significantly matched peptides. In contrast, standard scoring is the sum of the MS/MS ion scores of all non-duplicate peptides regardless of their absolute values. Thus, a protein can pass the significance threshold if it has enough low scoring peptides, even though none of the peptides themselves pass the significance threshold. By switching to standard scoring an increase in proteins yielding a total of 1898 and 1870 proteins were observed with a 762 protein overlap. This difference in matched proteins is quite drastic and the added identified proteins should be regarded as very tentative, even though they might have multiple peptides matched to the protein. The extreme case is obtained by disabling the require bold red option and utilizing standard scoring, this generated 11,159 and 10,107 identified proteins in the first and second sample with 9098 proteins overlapping both samples. Clearly, very drastic differences can be obtained by varying a few search criteria. A potential biomarker identified by the last two search criteria should be regarded as very tentative or, in most cases, unlikely. Furthermore, it is of outermost importance to identify a protein in multiple biological replicates to further minimize false positive matches. The proteins identified using the different search criteria discussed earlier and detected in both the biological replicates are visualized in a bulls eye plot shown in Fig. 2(B). The 130 overlapping proteins that represent the centre of the bulls eye plot are the statistically most significant proteins. These proteins have been further examined and are summarized in Table 1. Many of the identified proteins have multiple biological roles but they have been sorted by their primary function and class as given by the Uniprot database (www.uniprot.org). Special emphases have also been given to a function reported in Uniprot of being a marker for degenerative or regenerative processes. These proteins have been marked "indication of trauma" in the table. About 45% of the proteins listed have some reported function involved with degenerative/regenerative processes. However, some of the proteins such as cystatin-C, alpha-1-antitrypsin and other housekeeping proteins are usually also detected in normal CSF and should not be regarded as to be related specifically to TBI. In order to assess how many potential biomarkers for TBI that could be detected with the HLL, a literature search was conducted and is summarized in Table 2 [18–35]. Only proteins reported to have a down/up-regulation in CSF or human brain tissue in relation to an inflicted trauma to the head are included in the table. Protein breakdown products have been disregarded, since shotgun proteomics cannot determine whether the peptides comes from the intact protein or is a breakdown product. Out of the 33 proteins reported in the literature, 14 were found in both samples, 3 were only detected in the first sample and 16 were not detected in either of the samples. Among the more well studied biomarkers candidates such as NSE, GFAP, MBP, CK-B and S-100β all except MBP were detected. Interestingly, as many as γ-, ε-, ζ/δ- and σ- of the 14-3-3 protein family were detected. This is a group of proteins that are usually not detected by MS based methods because of the very low concentration in CSF. In general, the proteins that have in numerous studies shown to be involved in TBI pathology have been detected. Moreover, the proteins in Table 2 that are not detected might not be due to the actual method itself but by the time point the sample was taken, since the secondary molecular events in post-TBI trauma can yield temporally differentially expressed protein patterns. In comparison to other proteomic studies of the TBI proteome that have employed similar search criteria, our study have identified more than twice as many proteins [22,36]. The higher numbers of identified proteins are likely due to the compression of the dynamic range and hence detection of more low abundant proteins that is possible with HLL treatment.

Finally, 24 of the detected proteins were plotted against their reference concentration interval in normal CSF to obtain an overview of how well the compression of the dynamic range of the protein concentrations in CSF by HLL preparation was achieved (Fig. 3) [37,38]. The dynamic range of CSF, known to span at least 10 orders of magnitude, tends to correlate well with the experimental findings. Among the detected proteins was albumin as the most normally abundant at 0.2–0.6 mg/mL, down to the 14-3-3 protein family occurring at approximately 0.2 pg/mL, which represent a natural dynamic range of 9 orders of magnitude. This study shows the possibility for the detection of proposed biomarker candidates using a large sample load. However, for diagnostic purpose, the quantitative amount of each biomarker is of more interest. Such quantification studies should also be possible to perform in combination with HLL as long as the beads are not saturated.

4. Conclusions

The use of HLL shows the possibility for the capture and enrichment of protein biomarkers for TBI over a wide dynamic range. The most commonly reported protein biomarkers for TBI, such as NSE, GFAP, MBP, CK-B and S-100β as well as many other were successfully detected. HLL might be used as a tool for screening of low abundant protein biomarkers in human CSF in order to prevent additional injuries resulting from secondary events in the post-traumatic period of TBI.

Acknowledgements

This research was supported by Uppsala Berzelii Technology Center for Neurodiagnostics, with financing from the Swedish Governmental Agency for Innovation Systems and the Swedish Research Council, both with grant number P29797-1. The Swedish Research Council (VR 621-2008-3562) are also greatly acknowledged for financial support.

Appendix A. Supplementary data

Supplementary data associated with this article can be found, in the online version, at doi:10.1016/j.jchromb.2010.05.036.

References

[1] A.J. Schneier, B.J. Shields, S.G. Hostetler, H. Xiang, G.A. Smith, Pediatrics 118 (2006) 483.
[2] A.K. Ottens, F.H. Kobeissy, E.C. Golden, Z.Q. Zhang, W.E. Haskins, S.S. Chen, R.L. Hayes, K.K.W. Wang, N.D. Denslow, Mass Spectrom. Rev. 25 (2006) 380.
[3] S. Holmin, J. Soderlund, P. Biberfeld, T. Mathiesen, Neurosurgery 42 (1998) 291.
[4] R. Raghupathi, Brain Pathol. 14 (2004) 215.
[5] S.I. Svetlov, S.F. Larner, D.R. Kirk, J. Atkinson, R.L. Hayes, K.K.W. Wang, J. Neurotrauma 26 (2009) 913.
[6] E. Boschetti, P.G. Righetti, Proteomics 9 (2009) 1492.
[7] R. Stéphane, G. Audrey, L. Sylvain, Proteomics Clin. Appl. 2 (2008) 428.
[8] S. Roche, A. Gabelle, S. Lehmann, Proteomics Clin. Appl. 2 (2008) 428.
[9] N.I. Govorukhina, A. Keizer-Gunnink, A.G.J. van der Zee, S. de Jong, H.W.A. de Bruijn, R. Bischoff, J. Chromatogr. A 1009 (2003) 171.
[10] T. Ichibangase, K. Moriya, K. Koike, K. Imai, Biomed. Chromatogr. 23 (2009) 480.
[11] L. Guerrier, P.G. Righetti, E. Boschetti, Nat. Protocols 3 (2008) 883.
[12] V. Thulasiraman, S.H. Lin, L. Gheorghiu, J. Lathrop, L. Lomas, D. Hammond, E. Boschetti, Electrophoresis 26 (2005) 3561.
[13] A. Castagna, D. Cecconi, L. Sennels, J. Rappsilber, L. Guerrier, F. Fortis, E. Boschetti, L. Lomas, P.G. Rigetti, J. Proteome Res. 4 (2005) 1917.
[14] L. Guerrier, S. Claverol, L. Finzi, F. Paye, F. Fortis, E. Boschetti, C. Housset, J. Chromatogr. A 1176 (2007) 192.
[15] L. Sennels, M. Salek, L. Lomas, E. Boschetti, P.G. Righetti, J. Rappsilber, J. Proteome Res. 6 (2007) 4055.
[16] C. D'Ambrosio, S. Arena, A. Scaloni, L. Guerrier, E. Boschetti, M.E. Mendieta, A. Citterio, P.G. Righetti, J. Proteome Res. 7 (2008) 3461.
[17] S.M. Ahn, R.J. Simpson, Proteomics Clin. Appl. 1 (2007) 1004.
[18] B.M. Bellander, S.K. Singhrao, M. Ohlsson, P. Mattsson, M. Svensson, J. Neurotrauma 18 (2001) 1295.
[19] R.P. Berger, T. Dulani, P.D. Adelson, J.M. Leventhal, R. Richichi, P.M. Kochanek, Pediatrics 117 (2006) 325.
[20] A. Chiaretti, A. Antonelli, R. Riccardi, O. Genovese, P. Pezzotti, C. Di Rocco, L. Tortorolo, G. Piedimonte, Eur. J. Paediatr. Neurol. 12 (2008) 195.
[21] A. Conti, Y. Sanchez-Ruiz, A. Bachi, L. Beretta, E. Grandi, M. Beltramo, M. Alessio, J. Neurotrauma 21 (2004) 854.
[22] W.M. Gao, M.S. Chadha, R.P. Berger, G.S. Omenn, D.L. Allen, M. Pisano, P.D. Adelson, R.S.B. Clark, L.W. Jenkins, P.M. Kochanek, J. Neurotrauma 24 (2007) 43.
[23] M. Grossetete, J. Phelps, L. Arko, H. Yonas, G.A. Rosenberg, Neurosurgery 65 (2009) 702.
[24] Y.Y. Han, J.A. Carcillo, R.A. Ruppel, P.D. Adelson, S.R. Wisniewski, M.J. Bell, K.L. Janesko, D.W. Marion, P.M. Kochanek, Pediatr. Res. 47 (2000) 332.
[25] R. Hausmann, R. Riess, A. Fieguth, P. Betz, Int. J. Legal Med. 113 (2000) 70.
[26] T. Hayakata, T. Shiozaki, O. Tasaki, H. Ikegawa, Y. Inoue, F. Toshiyuki, H. Hosotubo, F. Kieko, T. Yamashita, H. Tanaka, T. Shimazu, H. Sugimoto, Shock 22 (2004) 102.
[27] G.W. Hergenroeder, J.B. Redell, A.N. Moore, P.K. Dash, Mol. Diagn. Ther. 12 (2008) 345.
[28] M. Is, A. Coskun, G.Z. Sanus, T. Tanriverdi, A.M. Kafadar, H. Hanimoglu, N. Tanriover, F. Gezen, M. Uzan, J. Clin. Neurosci. 14 (2007) 1163.
[29] A.D. Kay, A. Petzold, M. Kerr, G. Keir, E. Thompson, J.A.R. Nicoll, J. Neurotrauma 20 (2003) 943.
[30] M.A. Satchell, Y.C. Lai, P.M. Kochanek, S.R. Wisniewski, E.L. Fink, N.A. Siedberg, R.P. Berger, S.T. DeKosky, P.D. Adelson, R.S.B. Clark, J. Cereb. Blood Flow Metab. 25 (2005) 919.
[31] P.M. Shore, R.P. Berger, S. Varma, K.L. Janesko, S.R. Wisniewski, R.S.B. Clark, P.D. Adelson, N.J. Thomas, Y.C. Lai, H. Bayir, P.M. Kochanek, J. Neurotrauma 24 (2007) 75.
[32] R. Siman, N. Toraskar, A. Dang, E. McNeil, M. McGarvey, J. Plaum, E. Maloney, M.S. Grady, J. Neurotrauma 26 (2009) 1867.
[33] A. Singhal, A.J. Baker, G.M.T. Hare, F.X. Reinders, L.C. Schlichter, R.J. Moulton, J. Neurotrauma 19 (2002) 929.
[34] M. Uzan, H. Erman, T. Tanriverdi, G.Z. Sanus, A. Kafadar, H. Uzun, Acta Neurochir. 148 (2006) 1157.
[35] M.J. Whalen, T.M. Carlos, P.M. Kochanek, S.R. Wisniewski, M.J. Bell, J.A. Carcillo, R.S.B. Clark, S.T. DeKosky, P.D. Adelson, J. Neurotrauma 15 (1998) 777.
[36] J. Hanrieder, M. Wetterhall, P. Enblad, L. Hillered, J. Bergquist, J. Neurosci. Methods 177 (2009) 469.
[37] A.F. Huhmer, R.G. Biringer, H. Amato, A.N. Fonteh, M.G. Harrington, Dis. Markers 22 (2006) 3.
[38] K.S. Shores, D.R. Knapp, J. Proteome Res. 6 (2007) 3739.